

SCIENTIFIC REPORTS



OPEN

Interaction between isoprene and ozone fluxes in a poplar plantation and its impact on air quality at the European level

Received: 21 December 2015

Accepted: 10 August 2016

Published: 12 September 2016

Terenzio Zenone¹, Carlijn Hendriks², Federico Brilli^{3,4}, Erik Fransen⁵, Beniamio Gioli⁶, Miguel Portillo-Estrada¹, Martijn Schaap² & Reinhart Ceulemans¹

The emission of isoprene and other biogenic volatile organic compounds from vegetation plays an important role in tropospheric ozone (O₃) formation. The potentially large expansion of isoprene emitting species (e.g., poplars) for bioenergy production might, therefore, impact tropospheric O₃ formation. Using the eddy covariance technique we have simultaneously measured fluxes isoprene, O₃ and of CO₂ from a poplar (*Populus*) plantation grown for bioenergy production. We used the chemistry transport model LOTOS-EUROS to scale-up the isoprene emissions associated with the existing poplar plantations in Europe, and we assessed the impact of isoprene fluxes on ground level O₃ concentrations. Our findings suggest that isoprene emissions from existing poplar-for-bioenergy plantations do not significantly affect the ground level of O₃ concentration. Indeed the overall land in Europe covered with poplar plantations has not significantly changed over the last two decades despite policy incentives to produce bioenergy crops. The current surface area of isoprene emitting poplars-for-bioenergy remains too limited to significantly enhance O₃ concentrations and thus to be considered a potential threat for air quality and human health.

Isoprenoids represent an important and abundant class of biogenic volatile organic compounds (BVOCs); isoprene (C₅H₈, 2-methyl-1,3-butadiene) comprises about half of the total BVOCs emitted globally¹. Reactive isoprenoids in the atmosphere, and in particular isoprene, feed the cycle NO–NO₂–O₃ that is responsible for the formation² and degradation³ of tropospheric ozone (O₃). A recent study⁴ showed a carbon assimilation reduction of up to 19% in *Pinus ponderosa* and *Citrus* plantations, as a result of deposition of O₃ to the canopy, while the estimated yield losses caused by elevated ground-level [O₃] ranged between 7% and 16% for agricultural crops⁵. Moreover, a modeling study⁶ has predicted that isoprene emissions would increase in Europe from 11.5 Tg C yr⁻¹ to 16.0 Tg C yr⁻¹ as a consequence of an assumed expansion of bioenergy crops, as poplar (*Populus*), with subsequent important increases in ground-level [O₃], affecting crop yields and human health. Poplars are well known to be strong emitters of isoprene^{7,8} and the emissions are highly light and temperature dependent^{9,10}. Isoprene emissions increase with temperature up to 40 °C¹⁰, even when carbon assimilation is declining¹¹. This uncoupling of isoprene emission from the photosynthetic process reinforces the theory that isoprene may protect plants against heat stress^{12,13}. The response of isoprene emission to increasing [O₃] has primarily been examined in laboratory experiments under controlled environments (i.e. by employing enclosures) that might not reflect real-life conditions. Moreover in most of these studies^{4,14–16} high concentrations of O₃ (100–300 ppb) were applied for a short term (i.e., days to weeks) to simulate stress. In particular, no long-term observations of isoprene emissions and O₃ fluxes under uncontrolled field conditions have been made so far. We therefore run simultaneous

¹Department of Biology, Centre of Excellence on Plant and Vegetation Ecology (PLECO), University of Antwerp, B-2610 Wilrijk, Belgium. ²TNO, Department of Climate, Air and Sustainability, P.O. Box 80015, 3508 TA, Utrecht, the Netherlands. ³National Research Council, Institute of Agro-Environmental and Forest Biology (IBAF-CNR), Via Salaria Km 29,300 – 00016 Monterotondo Scalo, Roma, Italy. ⁴National Research Council, Institute for Sustainable Plant Protection (IPSP-CNR), Via Madonna del piano 10, 50017, Sesto Fiorentino, Italy. ⁵StatUa Centre for Statistics, University of Antwerp, Prinsstraat 13, B-2000 Antwerp, Belgium. ⁶National Research Council, Institute of Biometeorology (IBIMET-CNR), Via G. Caproni 8, 50145, Firenze, Italy. Correspondence and requests for materials should be addressed to T.Z. (email: Terenzio.Zenone@uantwerpen.be)

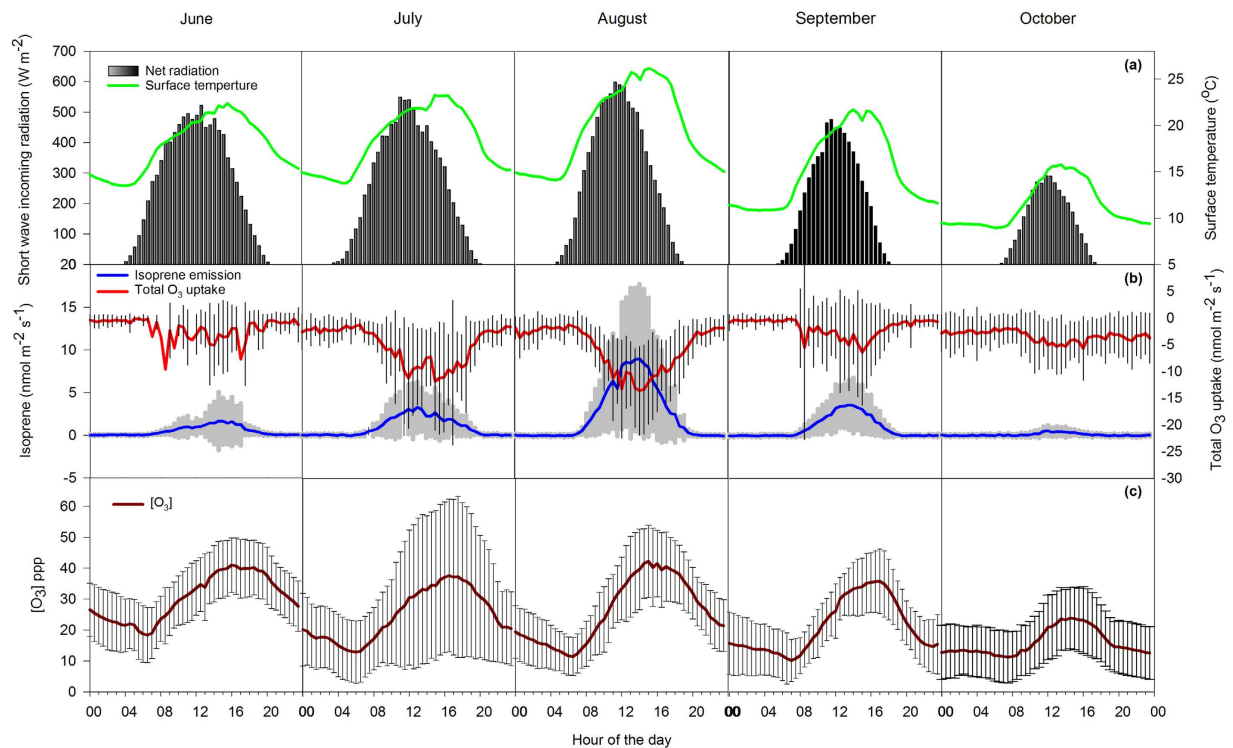


Figure 1. Diurnal cycles of (a) net radiation and surface temperature; (b) total O_3 uptake and isoprene fluxes and (c) $[\text{O}_3]$ concentrations. The diurnal cycles of fluxes represent averages calculated from the monthly half-hour eddy covariance data during the months June–October 2012.

ecosystem-level measurements of isoprene and O_3 fluxes by using the eddy covariance technique and investigated the influence of $[\text{O}_3]$ on both isoprene emission and total O_3 uptake.

In addition, we have scaled-up the measured isoprene emissions through the chemistry transport model (CTM) LOTOS-EUROS associated with the current surface area planted with poplar-for-bioenergy in Europe, as reported by the Food and Agriculture Organization of the United Nations¹⁷, and by the European Biomass Association¹⁸. This allowed us to quantify the potential impact of the isoprene fluxes on ground-level $[\text{O}_3]$.

Results

Experimental observations. Measured isoprene fluxes showed a well-defined daily cycle with maximum emission rates during the afternoon, from midday till 16.00 CEST (Fig. 1b), and corresponding with maximum values of incoming short-wave radiation (R_g) (Fig. 1a), while surface temperature (S_t) peaked about four hours later (Fig. 1a). Total O_3 uptake (Fig. 1b) also showed a diurnal trend that mirrored the isoprene fluxes and also occurred in parallel with increasing $[\text{O}_3]$ (Fig. 1c). Uptake of O_3 was dominated by the stomatal component (Supplementary information Fig. S3) that represented 70% of the total O_3 uptake. When looking at the entire season, isoprene fluxes were characterized by a remarkable peak emission occurring for a few days in August with the highest values reaching $38.6 \text{ nmol m}^{-2} \text{ s}^{-1}$ on 18 August 2012 and $38.0 \text{ nmol m}^{-2} \text{ s}^{-1}$ on 19 August 2012 (Fig. 2d). During these days (Fig. 2, shaded area), an increment of about 10°C (around midday) in both S_t and Air_t (Fig. 2a), an increase in the fluxes of latent heat (LE) (Fig. 2b) and of stomatal O_3 uptake (Fig. 2d), as well as a simultaneous decrease in the fluxes of sensible heat (H) (Fig. 2b) were observed. Despite these changes, R_g (Fig. 2a), gross primary production (GPP) and net ecosystem exchange (NEE) (Fig. 2c) did not show any significant change during the month of August 2012.

The Pearson correlations were computed between isoprene fluxes, O_3 uptake, $[\text{O}_3]$, R_g , radiation and Air_t (Table 1). The largest correlation for O_3 uptake was observed with $[\text{O}_3]$ ($r = 0.49$). The effects of $[\text{O}_3]$, R_g and Air_t on either O_3 uptake or isoprene fluxes were assessed using general linear models (GLM), revealing that $[\text{O}_3]$, R_g and Air_t had a highly significant effect on both O_3 uptake and isoprene fluxes. Based upon the GLM, we calculated the fraction of the variance of either isoprene fluxes or O_3 uptake attributable to $[\text{O}_3]$, R_g and Air_t , respectively (Table 2). A GLM that considers only R_g and Air_t explained 16.6% of the variance of O_3 uptake. Adding $[\text{O}_3]$ to the same model increased the r^2 from 0.166 to 0.287. Furthermore, a GLM that takes into account only $[\text{O}_3]$ explained 24.4% of the variance in O_3 uptake. As for isoprene fluxes, when the GLM included both R_g and Air_t , it was able to explain 54% of the variance. In particular, by adding $[\text{O}_3]$ to the same GLM (that already included both R_g and Air_t), the variance explained for isoprene fluxes increased by just 1% (from 54 to 55%). On the other hand, a GLM that considered only $[\text{O}_3]$ explained 21% of the variance in isoprene fluxes.

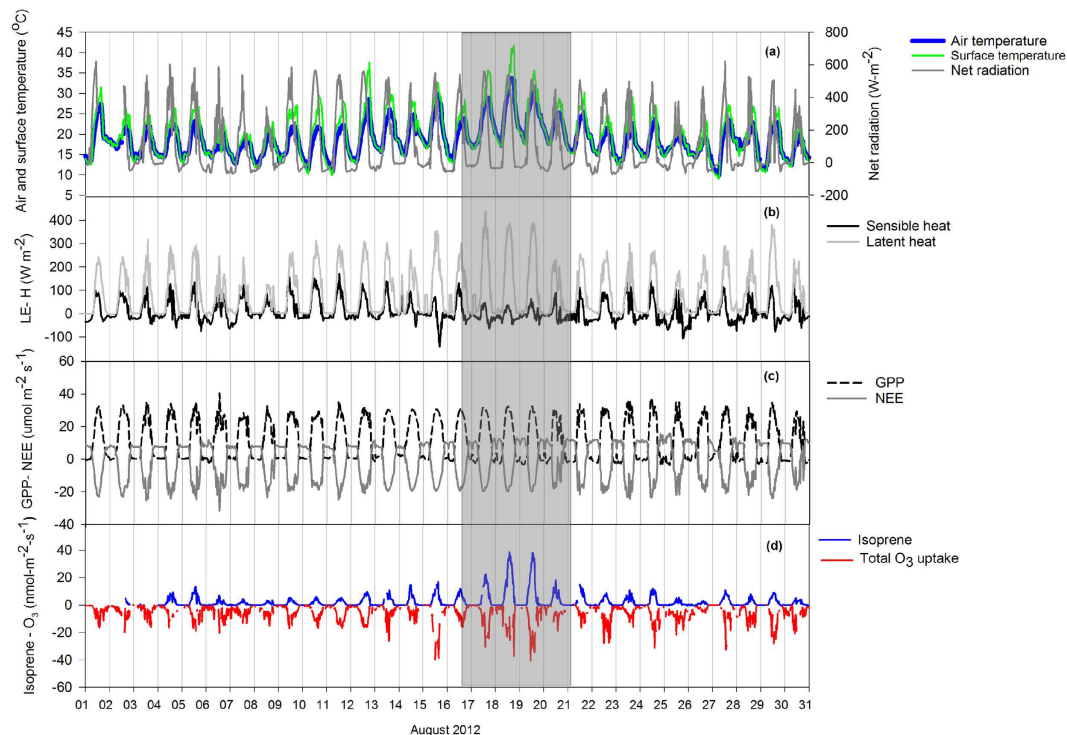


Figure 2. Average daily variation measured during August 2012 of (a) net radiation, air temperature and surface temperature; (b) energy exchange as latent heat (LE) and sensible heat (H); (c) CO_2 flux as net ecosystem exchange (NEE) and gross primary production (GPP); and (d) isoprene emission and total O_3 uptake. The shaded area represents the days characterized by a peak of isoprene emission.

Variable	Pearson correlation (r)				
	log(isoprene emission)	log(O_3 uptake)	$[O_3]$	Rg	Air _t
log(isoprene emission)	1	0.45	0.46	0.59	0.65
log(O_3 uptake)	0.45	1	0.49	0.32	0.36
$[O_3]$	0.46	0.49	1	0.34	0.55
Rg	0.59	0.32	0.34	1	0.45
Air _t	0.65	0.36	0.55	0.45	1

Table 1. Pearson correlation coefficients of the investigated variables. For isoprene emission and ozone uptake Pearson correlations of the log-transformed values were calculated since these variables were highly non-normal. This log transformation reversed the sign of the correlations for O_3 uptake. log(isoprene emission) = logarithm of isoprene emission ($nmol\ m^{-2}\ s^{-1}$). log(O_3 uptake) = logarithm of O_3 uptake ($nmol\ m^{-2}\ s^{-1}$). O_3 uptake = total ozone uptake ($nmol\ m^{-2}\ s^{-1}$). $[O_3]$ = ozone concentration (ppb). Rg = short-wave incoming radiation ($W\ m^{-2}$). Air_t = air temperature ($^{\circ}C$).

Model outcome	Variable	r^2
log(- O_3 uptake)	Air _t + Rg + $[O_3]$	0.28
	Air _t + Rg	0.16
	Difference by $[O_3]$	0.12*
	$[O_3]$	0.24
log(isoprene Fc)	Air _t + Rg + $[O_3]$	0.55
	Air _t + Rg	0.54
	Difference by $[O_3]$	0.01*
	$[O_3]$	0.21

Table 2. Correlation coefficients (r^2 values) for the GLM with the log(- O_3 uptake) and log(isoprene Fc) as dependent variables, and $[O_3]$, short-wave incoming radiation, (Rg) and air temperature (Air_t) as independent variables. *Partial r^2 gained by including $[O_3]$ in the model.

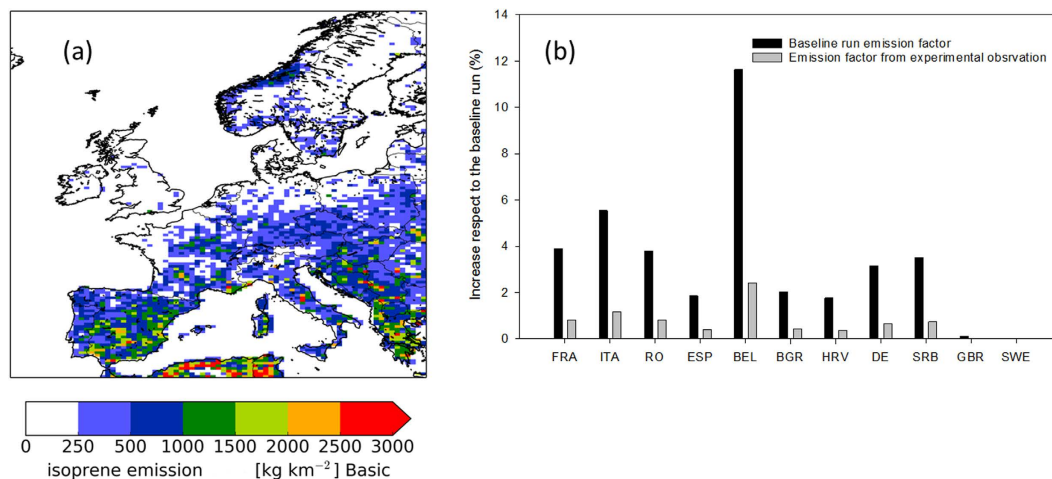


Figure 3. Isoprene emissions in Europe simulated by the LOTOS-EUROS model: (a) isoprene emission distribution for the basic run; (b) increase in isoprene emissions (in %) for an increased land surface area of poplar plantations and using emission factors extracted from measurements of this study (poplar-emisfac). The map was generated using the LOTOS-EUROS model version 1.10.005. URL link: www.lotos-euros.nl.

Model simulations. Simulated isoprene and O₃ fluxes were validated against the observations by running the LOTOS-EUROS model in which the vegetation of the entire 0.125 × 0.0625 degree grid cell, where the experimental site is located, was set to poplar plantation (run ‘Basic-zoom’). Since in our study case the resulting footprint for the flux measurements was entirely covered by poplars, this approach gave a fair comparison between simulated and measured fluxes of O₃ and isoprene.

The comparison between observed and simulated [O₃] as well as the comparison between observed and simulated O₃ uptake showed a reasonable agreement (SI Fig. S1). However, fast fluctuations in O₃ fluxes (especially deposition peaks) were not captured well by the LOTOS-EUROS model as the underestimation of O₃ fluxes mainly occurred at times when the O₃ fluxes were very large for a short while. On average, LOTOS-EUROS overestimated the O₃ flux by 22%. The comparison between modeled and observed isoprene fluxes (SI Fig. S4) showed that the model underestimated the seasonal variability of isoprene emissions in late summer (August and September) whereas the observed emissions were overestimated in June. A comparison between simulated and observed [O₃] from 47 rural sites belonging to the European Monitoring and Evaluation Programme EMEP (SI Fig. S2) showed an average model bias of 2.7 ppb with an average hourly temporal coefficient of determination (*r*²) of 0.59 throughout all the stations. When model simulations of the [O₃] daily maxima were compared to the observations, a better agreement with an average bias of 0.67 ppb and an *r*² of 0.76: the slopes of both plots (0.74 and 0.77 for average and daily maximum respectively) indicate that LOTOS-EUROS underestimates the spatial variability and daily maximum [O₃] (SI Fig. S2).

Isoprene fluxes obtained using the basic configuration of the LOTOS-EUROS chemistry transport model with a resolution of 0.5 × 0.25 degrees and the land use database CORINE 2006 (ID run named “basic” in SI Table 2) showed that the largest emissions were associated with isoprene emitting forests (Fig. 3a). The north-south gradient in isoprene emission rates reflected the temperature gradient across Europe, as southern Mediterranean areas feature the highest temperatures with respect to Northern ones. After incorporating into the LOTOS-EUROS model the areas covered by poplar plantations as reported by the FAO for the different countries in Europe (Table S3) and selecting the vegetation-specific isoprene emission factor for poplar plants (ID run “poplar” in SI Table 2) isoprene fluxes increased from 0.01% to 11.6% compared to the “basic” run. However, when a vegetation-specific isoprene emission factor obtained from the present experimental observations was applied to LOTOS-EUROS (ID run named “poplar emission factor” in SI Table 2), total isoprene emissions were 26% lower compared to the LOTOS-EUROS basic configuration and a maximum increase of 2.4% of the isoprene emissions was obtained (Fig. 3b). Overall, the simulated isoprene fluxes increased from 3.4 to 3.5 Tg C for the period of April–October 2012 when the present surface area of poplar plantations was included in LOTOS-EUROS model by using the vegetation-specific isoprene emission factor obtained in our observations.

In this study, the isoprene concentration pattern (Fig. 4a) mapped the actual distribution of isoprene emissions in Europe: indeed very low concentrations (<1 ppb) were displayed in north-western Europe whereas in southern Europe concentrations reached 2–3 ppb. Differently from isoprene concentrations, [O₃] (Fig. 4b) ranged between 20 and 50 ppb for central Europe. The lowest levels of [O₃] are found in regions with high NO_x levels such as central England, the Ruhr area in Germany, the Netherlands and the Paris region in France, where ozone titration during the night plays an important role. [O₃] generally increase towards southern Europe, with the highest values found along the Mediterranean coast. When poplar plantations were included in the land-use map, an increase in [O₃] ranging from 0.025 to 0.15 ppb (Fig. 4d) was observed in areas where poplar plantations were located, caused by an increase of isoprene concentrations from 0.02 to 0.06 ppb (Fig. 4c). The increase in [O₃] highlighted in Fig. 4c represents the net impact of the isoprene fluxes emitted by poplar plantations: overall [O₃] increased by 0.1–0.5% while O₃ deposition in poplars increased by 0.1–0.3%.

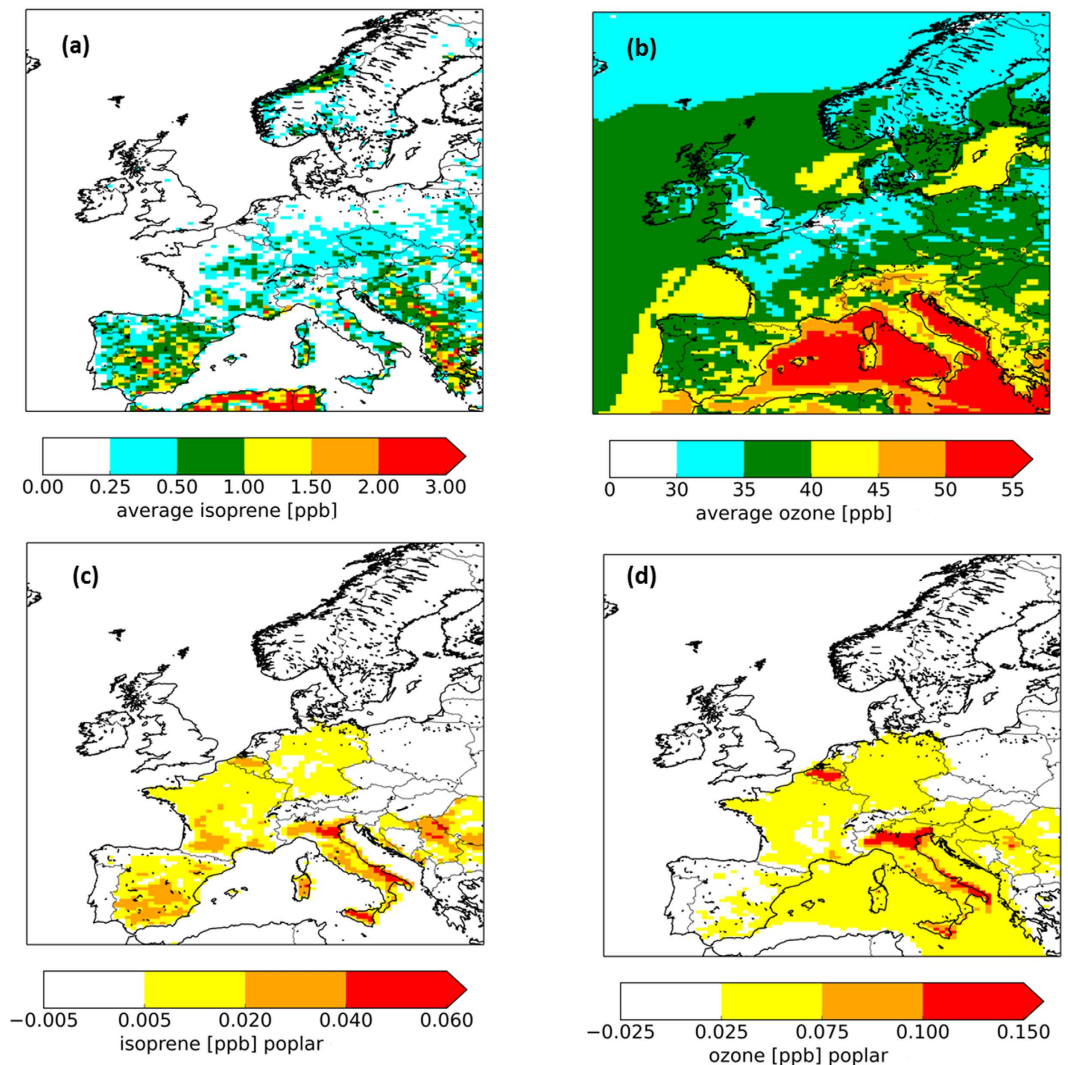


Figure 4. Average concentrations for the period April - September 2012 as simulated by the LOTOS-EUROS model, basic run for isoprene (a) ozone (b); and the difference (in ppb) caused by an increase in poplar plantation area for isoprene (c) and $[O_3]$ (d). The map was generated using the LOTOS-EUROS model version 1.10.005. URL link: www.lotos-euros.nl.

Discussion

The highest isoprene fluxes observed in this study occurred in mid-August 2012 (Fig. 1), when isoprene synthase activity was maximized by the increase of the air and surface temperatures under high light intensities in a fully developed canopy where strong isoprene emitting adult leaves outweighed the young ones¹⁹. As the poplars were not water stressed²⁰ during the whole growing season, they kept their stomata open and increased the fluxes of evapotranspiration in an attempt to reduce the leaf temperature, although the cooling effect due to isoprene emission was negligible (as it accounted for only 0.1–0.3% of the cooling effect of water). Because the amount of R_g did not change (during the measurements period), fluxes of H decreased simultaneously to increased LE, causing the observed reduction of the Bowen ratio. However, GPP and NEE were not affected by this thermal variation; therefore poplar plants emitted isoprene at high rates in the field when the photosynthetic machinery resulted undamaged by stress. This evidence further suggests that isoprene makes the chloroplasts membranes more resistant and more performing under high temperatures as observed in the past¹², also in laboratory trials²¹. Indeed, experiments employing *Populus* grown in pots²² have evidenced the role of isoprene in unstressed plants, as the chloroplasts of isoprene emitting plants dissipated less energy as heat than the chloroplasts of non-emitting plants, when exposed to physiologically high temperatures (29–38 °C) that did not damage the photosynthetic apparatus. While the process of isoprene emission is crucial for tropospheric O_3 formation in the atmosphere, the $[O_3]$ itself also has important consequences on the physiology of plants by creating a feedback loop that influences the production and emission of isoprene⁴. Nevertheless, the response of isoprene emission to $[O_3]$ may vary considerably and is related to the level and the duration of the O_3 exposure. It has been hypothesized^{4,23} that the response of isoprene emission to increasing doses of $[O_3]$ follows the most common form of the hormetic dose-response curve. The effect of moderate $[O_3]$ on isoprene emission has been investigated in *Populus nigra* plants in

a laboratory experiment¹⁵, which showed that the emission of isoprene and oxygenated six-carbon (C6) volatiles were inhibited when plants were exposed to an [O₃] of 80 ppb for two weeks. However, the impact of [O₃] on isoprene emission has been investigated in several other laboratory studies with conflicting results: some studies highlighted that high doses of O₃ enhanced isoprene emission^{15,23,24}, whereas others^{25–27} reported an inhibition of isoprene emission in poplars under more usual low doses of [O₃].

The experimental observations of isoprene and O₃ fluxes were used, through the application of the LOTOS-EUROS model, to investigate to what extent existing poplar plantations influence ground level [O₃] and found their impact to be small. Our results show that isoprene fluxes affected the average [O₃] during the period April–September (2012) by max. 0.5%, thus indicating that the poplar plantations currently in place for biomass production do not significantly alter the [O₃]. The slight increase in [O₃] was also partially counteracted by the increased O₃ deposition; poplars are characterized by high LAI and are effective O₃ sinks²⁸.

The maximum effect of isoprene emission on [O₃] was calculated using the highest emission factor (60 μg gDM⁻¹ hr⁻¹) regarding isoprene emission from poplar trees reported in the literature, where it was found to range between 45 and 60 μg gDM⁻¹ hr⁻¹^{18,29,30}. However, both the isoprene emission factor and leafy biomass derived from our experimental observations provides a 26% lower total isoprene emission than that resulted from LOTOS-EUROS model in the basic configuration. A misrepresentation of the seasonal variability of isoprene emissions in LOTOS-EUROS caused an underestimation of observed isoprene fluxes in September. This bias influenced O₃ production in the model, but since peaks of [O₃] mainly occurred before September 2012, the impact on our conclusions is expected to be small. The observations presented here are representative for the northern temperate climate zone of Europe, which contains the countries with the highest area of poplar plantations (SI Table 3). Since the relationship used in LOTOS-EUROS model to simulate isoprene emissions from poplar plantations on the basis of the observations is temperature-dependent³⁰, LOTOS-EUROS produced reliable results for the rest of Europe. On the other hand, the isoprene emission factor representing the agricultural land employed here to run the LOTOS-EUROS model is lower than that used by both Ashworth *et al.*³¹ and Lathière *et al.*³². This means that the impact of poplar plantations on the [O₃] simulated in our study may be relatively high considering that isoprene emission factor and leafy biomass quantities of poplars used in LOTOS-EUROS are on the high end of the values reported in literature. However, total isoprene emission resulting from our study was lower than that reported in e.g. Ashworth *et al.*⁶ which accounted for 11.5 Tg C yr⁻¹ while in Beltman *et al.*³³ it was estimated to be 5 Tg C for the period April–September (2012). The differences in the estimates of isoprene emission between past studies and our present work are caused by differences in domain (in Ashworth *et al.*⁶ plantations expanded much further east) and by a diverse time period of analysis (only summertime has been considered in Beltman *et al.*³³, whereas the whole year in Ashworth *et al.*⁶). So far, simulations of isoprene fluxes from poplar plantations have mainly used future scenarios^{31–33}, where the impacts of isoprene emissions on [O₃] levels were driven by the assumption of a very large increment in both the area of poplar plantations and in the extent of the emission factor chosen to perform the simulations. Therefore, results from past simulations suggested that isoprene fluxes emitted from the foreseen increasing biomass production in expanding poplar-for-bioenergy plantations could potentially increase the risk of O₃ damage to human health, crops and ecosystems. As a consequence, to counteract the increasing level of tropospheric [O₃] might require a large investment for the abatement of NO_x³³. The impact of domestic biomass production for fuel and power generation needed to meet EU targets for 2020 regarding the [O₃] is small, but significant (Ashworth *et al.*⁶). In particular, the study of Ashworth *et al.* (2012)⁶ assumed that 72 Mha of poplar were to be planted to meet the projected use of biomass as a renewable energy source, leading to a 39% increase in isoprene emissions. Moreover other authors³⁴ suggested that, especially in eastern Europe, a large proportion of agricultural land might have been converted into biomass forest.

However, despite policies encouraging the use of biomass for energy are already in place³⁵, data from the literature confirmed the trend that the area covered by poplar plantations did not show any significant changes over the last 20 years, at least in the countries considered in our study (ref. 17, Table S3). The current area of poplar SRC plantations present in Europe (Table S4) is far too small to create a threat for O₃ formation, leading to only 1% extra isoprene emissions, as demonstrated by our simulation. If anthropogenic emissions of non-methane volatile organic compounds (NMVOC) are underestimated in our model study, which is not unlikely as these emissions are quite uncertain, the impact of isoprene emissions on O₃ formation calculated here could be overestimated. Hence, our study indicates that increasing the production of bioenergy from poplar plantations in Europe would not reduce the air quality in the short-term; therefore policymakers should not be concerned in supporting policies that encourage the planting of bioenergy crops.

Material and Methods

The research site was a poplar (*Populus*) bioenergy plantation located in Lochristi, East-Flanders (Belgium; 51°06′44″N, 3°51′02″E) at an elevation of 6 m above sea level. The plantation was established in April 2010 with 12 selected clones of *Populus deltoides*, *P. maximowiczii*, *P. nigra*, and *P. trichocarpa*, at a density of 8000 plants ha⁻¹ on a surface of 18.4 ha. The main environmental conditions and stand characteristics are reported in Table S1. The research site was equipped with two different eddy covariance (EC) systems. One system was used to monitor the CO₂, latent heat (*LE*), sensible heat (*H*) and O₃ fluxes between the ecosystem and the atmosphere and comprised a three-dimensional sonic anemometer (model CSAT3, Campbell Scientific, Logan, UT, USA) to measure the wind speed components, a fast response LOZ-3F O₃ analyzer (Drummond Technology Inc., Ontario, Canada) and a fast response CO₂/H₂O infrared analyzer (LI-7000, LI-COR, Lincoln, NE, USA). The LOZ-3F O₃ analyzer is based on chemi-luminescence with Eosin-Y dye circulated continuously through a peristaltic pump in the sample cell, and it measures the O₃ mixing ratio at a 10 Hz sampling frequency. A slow response O₃ analyzer (API 400E, Teledyne Instruments, CA, USA) was used to continuously monitor [O₃], which was then compared with the concentrations measured by the LOZ-3F, to determine whether any drifting had occurred in the signal

of the LOZ-3F. The API instrument was calibrated every six months by the Flemish Environment Agency (www.vmm.be). The second EC system monitored the fluxes of biogenic volatile organic compounds (BVOCs) and included a sonic anemometer (model USA1, Metek GmbH, Elmshorn, Germany) coupled with a proton transfer reaction “Time-of-Flight” mass spectrometer (PTR-TOF-MS) (Ionicon, Innsbruck, Austria) that measured the volume mixing ratios (VMRs) of BVOCs. The data streams of the anemometer and the PTR-TOF-MS were acquired independently by two different computers and synchronized with dedicated software (NTP, Network Time Protocol, University of Delaware, DE, USA) to an independent external clock through the internet, with an accuracy of <20 ms. The two EC systems were completely independent, although they were installed very close to each other with a 1 m spatial separation between the inlets of the two sampling lines.

Fluxes of O₃ were calculated using EddyPro (version 5.2.0): the mean lateral and vertical velocity components were forced to zero by a two-component rotation. The maximum cross covariance function (within the 30-min averaging time) was used to determine the lag time for O₃, which was about 2 s. A frequency response correction was performed according to Moncrieff *et al.*³⁶.

The fluxes of CO₂ and of water vapor were calculated using the EdiRe software (R. Clement, University of Edinburgh, UK; www.geos.ed.ac.uk/abs/research/micromet/EdiRe/).

In order to reduce the burden of PTR-TOF-MS data analysis, the overall raw dataset collected during the measuring campaign was post-processed by the routine programs of Müller *et al.*³⁷ to screen for the presence of emitted/deposited fluxes of the most common protonated ions unambiguously found to be related to a BVOC. After post-processing, PTR-TOF-MS data were background corrected by subtracting ambient VOC-free air generated by a gas calibration unit (GCU) (Ionimed, Innsbruck, Austria) and calibrated regularly with the same gas standard (Apel Riemer, USA) during the length of the field campaign to quantify the VMRs of the selected BVOCs. This latter technique has been previously described in detail¹¹. In order to standardize the computation of isoprene fluxes with the EC method the EddyPro software was modified into a new customized version that was named EddyVoc. Similarly to EddyPro, the processing routine programmed in EddyVoc masked the raw data with a quality flag to exclude individual spikes, values out-of-range and background calibration periods of the PTR-TOF-MS. Further details about the EC data processing were provided previously (Brilli *et al.*¹¹).

Estimation of stomatal O₃ fluxes. Stomatal resistance to water vapor (R_{sto} , Eq. 1) was calculated from the EC measured evapotranspiration using the evaporative/resistance method³⁸:

$$R_{sto} = \frac{c_p * \rho * VPD}{\lambda * \gamma * E_L} - (R_a + R_b) \quad [1]$$

where λ is the latent heat of vaporization in air (J kg⁻¹), γ is the psychrometric constant (0.065 kPa K⁻¹), E_L is the transpiration rate (kg H₂O m⁻² s⁻¹) after subtracting the evaporative contribution from the soil, c_p is the specific heat of air (J kg⁻¹ K⁻¹), ρ (kg m⁻³) is the density of dry air, VPD is the vapor pressure deficit at leaf level (kPa), R_a and R_b (s m⁻¹) are the aerodynamic, respectively, laminar sublayer resistances. Stomatal conductance to ozone was calculated as the inverse of R_{sto} corrected for the difference in diffusivity between O₃ and water vapor. Stomatal O₃ flux was calculated by multiplying the stomatal conductance to O₃ by [O₃] assuming that inter-cellular [O₃] was zero.

Statistical analysis. To investigate the influence of [O₃] on the isoprene emission and the total O₃ uptake we used a correlation and a regression model approach. Due to the skewed distribution of the O₃ uptake and isoprene emissions, these variables were logarithmically transformed to be used as outcome variable in the regression analysis. Since the logarithms of a negative number cannot be calculated, we calculated the log(-O₃ uptake+1) and log(isoprene emission + 3) respectively. These log-transformed values were used to calculate Pearson correlation (r) coefficients. For the multivariable linear regression models [O₃], R_g , and Air_t were entered as independent variables. The log-transformed values of either isoprene emission or O₃ uptake was entered as dependent variable.

Calculation of the partial r^2 for [O₃] in the model with either isoprene emission or O₃ uptake, was carried out comparing the R^2 between a regression model with [O₃], R_g , and Air_t and a regression model with only R_g , and Air_t . The difference in r^2 between these two models represents the fraction of the variance in the outcome (either isoprene emission or O₃ uptake) that can only be attributed to [O₃]. Linear regression models were fitted using the lm() function in the statistical software package R, version 3.1.2.

The CTM LOTOS-EUROS model. The LOTOS-EUROS v1.10 is a 3-D regional chemistry transport model that simulates air pollution in the lower troposphere. For a more detailed description of the model reference is made to Schaap *et al.*³⁹. The model uses a normal longitude–latitude projection and allows the user to specify the resolution and domain within its master domain that encompasses Europe and its periphery. For this work, runs were performed at a 0.5 × 0.25 degree resolution for the European domain (15° E – 35° W, 30–60° N) and at 1/8 × 1/16 degree for a domain containing Belgium. The model ceiling is at 3.5 km above sea level and consists of three dynamical layers: a mixing layer and two reservoir layers above. The height of the mixing layer at each time and position is extracted from the ECMWF meteorological data used to drive the model. The height of the reservoir layers is set to the difference between the ceiling and mixing layer height. Both layers are equally thick with a minimum of 50 m. If the mixing layer is near or above 3500 m high, the top of the model exceeds 3500 m. A surface layer with a fixed depth of 25 m is included in the model to monitor ground-level concentrations.

Advection in all directions is handled with the monotonic advection scheme developed by Walcek⁴⁰. Isoprene chemistry and hydrolysis of N₂O₅ were described by Adelman⁴¹ and by Schaap *et al.*⁴², respectively. Stomatal resistance is described by the parameterization of Emberson *et al.*⁴³ and the aerodynamic resistance is calculated for all land-use types separately. Isoprene emissions were calculated based on detailed information about tree

types in Europe: a land use dataset⁴⁴ was combined with the distributions of 115 tree species over Europe²⁹. During each simulation time step, isoprene emissions, for each grid cell, were calculated as a function of the biomass density and standard emission factor of the species or land-use class, taking into account the growing season of deciduous trees and agricultural crops. Moreover, the role of the local temperature and photosynthetically active radiation were taken into account in the biogenic emissions by following the empirically designed algorithms described by Guenther *et al.*³⁰. Anthropogenic emissions were taken from the TNO-MACC database⁴⁵ which is a widely used emission database for air quality modelling. Emission totals and trends reported in the TNO-MACC database are in line with what is reported in other emission databases for Europe^{46,47}. The model set-up used here did not contain secondary organic aerosol formation or a volatility basis set approach. The different model runs were analyzed and compared in terms of isoprene emissions, isoprene and O₃ concentrations. Modeled O₃ concentrations were validated using measured concentrations from the European Monitoring and Evaluation Programme (EMEP) monitoring network (www.emep.int). Only background stations situated in rural areas below 700 m height were considered.

References

- Guenther, A. B. *et al.* The model of emissions of gases and aerosols from nature version 2.1 (MEGAN2.1): an extended and updated framework for modeling biogenic emissions. *Geosci Model Dev* **5**, 1471–1492, doi: 10.5194/gmd-5-1471-2012 (2012).
- Jardine, K. J. *et al.* Within-plant isoprene oxidation confirmed by direct emissions of oxidation products methyl vinyl ketone and methacrolein. *Global Change Biol* **18**, 973–984 (2012).
- Rivera-Ríos, J. C. *et al.* Conversion of hydroperoxides to carbonyls in field and laboratory instrumentation: Observational bias in diagnosing pristine versus anthropogenically controlled atmospheric chemistry. *Geophys Res Lett* **41**, 8645–8651, doi: 10.1002/2014GL061919 (2014).
- Calfapietra, C., Fares, S. & Lofeto, F. Volatile organic compounds from Italian vegetation and their interaction with ozone. *Environ Pollut* **157**, 1478–1486, doi: 10.1016/j.envpol.2008.09.048 (2009).
- Van Dingenen, R. *et al.* The global impact of ozone on agricultural crop yields under current and future air quality legislation. *Atmos Environ* **43**, 604–618, doi: 10.1016/j.atmosenv.2008.10.033 (2009).
- Ashworth, K., Wild, O. & Hewitt, C. N. Impacts of biofuel cultivation on mortality and crop yields. *Nat Clim Change* **3**, 492–496, doi: 10.1038/Nclimate1788 (2013).
- Guidolotti, G., Calfapietra, C. & Loreto, F. The relationship between isoprene emission, CO₂ assimilation and water use efficiency across a range of poplar genotypes. *Physiol Plantarum* **142**, 297–304, doi: 10.1111/j.1399-3054.2011.01463.x (2011).
- Kesselmeier, J. & Staudt, M. Biogenic volatile organic compounds (VOC): An overview on emission, physiology and ecology. *J Atmos Chem* **33**, 23–88, doi: 10.1023/A:1006127516791 (1999).
- Loreto, F., Harley, P. C., Dimarco, G. & Sharkey, T. D. Estimation of mesophyll conductance to CO₂ flux by three different methods. *Plant Physiol* **98**, 1437–1443, doi: 10.1104/Pp.98.4.1437 (1992).
- Monson, R. K. *et al.* Relationships among isoprene emission rate, photosynthesis, and isoprene synthase activity as influenced by temperature. *Plant Physiol* **98**, 1175–1180, doi: 10.1104/Pp.98.3.1175 (1992).
- Brilli, F. *et al.* Simultaneous leaf- and ecosystem-level fluxes of volatile organic compounds from a poplar-based SRC plantation. *Agr Forest Meteorol* **187**, 22–35, doi: 10.1016/j.agrformet.2013.11.006 (2014).
- Singsaas, E. L., Lerdau, M., Winter, K. & Sharkey, T. D. Isoprene increases thermotolerance of isoprene-emitting species. *Plant Physiol* **115**, 1413–1420 (1997).
- Vickers, C. E., Gershenzon, J., Lerdau, M. T. & Loreto, F. A unified mechanism of action for volatile isoprenoids in plant abiotic stress. *Nat Chem Biol* **5**, 283–291, doi: 10.1038/Nchembio.158 (2009).
- Velikova, V., Tsonev, T., Pinelli, P., Alessio, G. A. & Loreto, F. Localized ozone fumigation system for studying ozone effects on photosynthesis, respiration, electron transport rate and isoprene emission in field-grown Mediterranean oak species. *Tree Physiol* **25**, 1523–1532 (2005).
- Fares, S. *et al.* Impact of high ozone on isoprene emission, photosynthesis and histology of developing *Populus alba* leaves directly or indirectly exposed to the pollutant. *Physiol Plantarum* **128**, 1456–465, doi: 10.1111/j.1399-3054.2006.00750.x (2006).
- Fares, S., Loreto, F., Kleist, E. & Wildt, J. Stomatal uptake and stomatal deposition of ozone in isoprene and monoterpene emitting plants. *Plant Biology* **10**, 44–54, doi: 10.1055/s-2007-965257 (2008).
- FAO. 24th Session of the International Poplar Commission and 46th Session of its Executive Committee. Improving lives with poplars and willows. Synthesis of Country Progress Reports. Dehradun, India, 29 October–2 November 2012. FO: IPC/12/REP. Food and Agriculture organization of the United Nations. Rome, January 2013.
- Dimitriou, I. *et al.* “Quantifying environmental effects of short rotation coppice (SRC) on biodiversity, soil and water”. *IEA Bioenergy Task* **43** No. 2011 2011.
- Brilli, F. *et al.* Rapid leaf development drives the seasonal pattern of volatile organic compound (VOC) fluxes in a ‘coppiced’ bioenergy poplar plantation. *Plant, Cell & Environment* **39**, 539–555, doi: 10.1111/pce.12638 (2016).
- Zenone, T. *et al.* Biophysical drivers of the carbon dioxide, water vapor, and energy exchanges of a short-rotation poplar coppice. *Agr Forest Meteorol* **209**, 22–35, doi: 10.1016/j.agrformet.2015.04.009 (2015).
- Velikova, V. *et al.* Increased thermostability of thylakoid membranes in isoprene-emitting leaves robbed with three biophysical techniques. *Plant Physiol* **157**, 905–916, doi: 10.1104/pp.111.182519 (2011).
- Pollastri, S., Tsonev, T. & Loreto, F. Isoprene improves photochemical efficiency and enhances heat dissipation in plants at physiological temperatures. *J Exp Bot* **65**, 1565–1570, doi: 10.1093/jxb/eru033 (2014).
- Loreto, F., Pinelli, P., Manes, F. & Kollist, H. Impact of ozone on monoterpene emissions and evidence for an isoprene-like antioxidant action of monoterpenes emitted by *Quercus ilex* leaves. *Tree Physiol* **24**, 361–367, doi: 10.1093/treephys/24.4.361 (2004).
- Fares, S., Oksanen, E., Lannepaa, M., Julkunen-Tiitto, R. & Loreto, F. Volatile emissions and phenolic compound concentrations along a vertical profile of *Populus nigra* leaves exposed to realistic ozone concentrations. *Photosynth Res* **104**, 61–74, doi: 10.1007/s1120-010-9549-5 (2010).
- Calfapietra, C., Mugnozza, G. S., Karnosky, D. F., Loreto, F. & Sharkey, T. D. Isoprene emission rates under elevated CO₂ and O₃ in two field-grown aspen clones differing in their sensitivity to O₃. *New Phytol* **179**, 55–61, doi: 10.1111/j.1469-8137.2008.02493.x (2008).
- Ryan, A., Cojocariu, C., Possell, M., Davies, W. J. & Hewitt, C. N. Defining hybrid poplar (*Populus deltoides* x *Populus trichocarpa*) tolerance to ozone: identifying key parameters. *Plant Cell Environ* **32**, 31–45, doi: 10.1111/j.1365-3040.2008.01897.x (2009).
- Calfapietra, C. *et al.* Isoprene synthase expression and protein levels are reduced under elevated O₃ but not under elevated CO₂ (FACE) in field-grown aspen trees. *Plant Cell Environ* **30**, 654–661, doi: 10.1111/j.1365-3040.2007.01646.x (2007).
- Erisman, J. W. *et al.* Parametrization of surface resistance for the quantification of atmospheric deposition of acidifying pollutants and ozone. *Atmospheric Environment* **28**, Issue 16, 2595–2607 (1994).
- Koble R. & Seufert G. Novel maps for forest tree species in Europe, Proceedings of the 8th European Symposium on the Physico-Chemical Behaviour of Air Pollutants: “A Changing Atmosphere!”, Torino (It), 17–20 September 2001.

30. Guenther, A. B., Zimmerman, P. R., Harley, P. C., Monson, R. K. & Fall, R. Isoprene and monoterpene emission rate variability - Model evaluations and sensitivity analyses. *J Geophys Res-Atmos* **98**, 12609–12617, doi: 10.1029/93jd00527 (1993).
31. Ashworth, K., Folberth, G., Hewitt, C. N. & Wild, O. Impacts of near-future cultivation of biofuel feedstocks on atmospheric composition and local air quality. *Atmos Chem Phys* **12**, 919–939, doi: 10.5194/acp-12-919-2012 (2012).
32. Lathiere, J. *et al.* Impact of climate variability and land use changes on global biogenic volatile organic compound emissions. *Atmos Chem Phys* **6**, 2129–2146 (2006).
33. Beltman, J. B., Hendriks, C., Tum, M. & Schaap, M. The impact of large scale biomass production on ozone air pollution in Europe. *Atmos Environ* **71**, 352–363, doi: 10.1016/j.atmosenv.2013.02.019 (2013).
34. Fischer, G. *et al.* Biofuel production potentials in Europe: Sustainable use of cultivated land and pastures, Part II: Land use scenarios. *Biomass Bioenerg* **34**, 173–187, doi: 10.1016/j.biombioe.2009.07.009 (2010).
35. Official Journal of the European Union 5/6/2009 Directive 2009/28/EC of the European Parliament and of the Council of 23 April 2009 on the promotion of the use of energy from renewable sources and amending and subsequently repealing Directives 2001/77/EC and 2003/30/EC.
36. Moncrieff, J. B. *et al.* A system to measure surface fluxes of momentum, sensible heat, water vapour and carbon dioxide. *J Hydrol* **189**, 589–611 (1997).
37. Müller, M., Mikoviny, T., Jud, W., D'Anna, B. & Wisthaler, A. A new software tool for the analysis of high resolution PTR-TOF mass spectra. *Chemometr Intell Lab* **127**, 158–165, doi: 10.1016/j.chemolab.2013.06.011 (2013).
38. Fares, S. *et al.* Ozone deposition to an orange orchard: Partitioning between stomatal and non-stomatal sinks. *Environ Pollut* **169**, 258–266, doi: 10.1016/j.envpol.2012.01.030 (2012).
39. Schaap, M. *et al.* The LOTOS-EUROS model: description, validation and latest developments. *Int J Environ Pollut* **32**, 270–290, doi: 10.1504/ijep.2008.017106 (2008).
40. Walcek, C. J. Minor flux adjustment near mixing ratio extremes for simplified yet highly accurate monotonic calculation of tracer advection. *J Geophys Res-Atmos* **105**, 9335–9348, doi: 10.1029/1999jd901142 (2000).
41. Adelman, Z. E. *A reevaluation of the carbon bond-IV photochemical mechanism* M.Sc. thesis, University of North Carolina (1999).
42. Schaap, M. *et al.* Anthropogenic black carbon and fine aerosol distribution over Europe. *J Geophys Res-Atmos* **109**, doi: 10.1029/2003jd004330 (2004).
43. Emberson, L. D., Ashmore, M. R., Simpson, D., Tuovinen, J. P. & Cambridge, H. M. *Towards a model of ozone deposition and stomatal uptake over Europe*. EMEP/MSC-W 6/2000. 57 pp (Norwegian Meteorological Institute, Oslo, Norway, 2000).
44. Büttner, G., Kosztra, B., Maucha, G. & Pataki, R. *Implementation and achievements of CLC2006*. (European Topic Centre Land Use and Spatial Information/European Environment Agency, 2012).
45. Kuenen, J., Denier van der Gon, H., Visschedijk, A., Van der Brugh, H. & Van Gijlswijk, R. *MACC European emission inventory for the years 2003–2007*. (Utrecht, 2011).
46. Granier, C. *et al.* Evolution of anthropogenic and biomass burning emissions of air pollutants at global and regional scales during the 1980–2010 period. *Climatic Change*, **109**(1–2), 163–190 (2011).
47. Kuenen, J. J. P. *et al.* TNO-MACC_II emission inventory; a multi-year (2003–2009) consistent high-resolution European emission inventory for air quality modelling. *Atmos. Chem. Phys.* **14**, 10963–10976 doi: 10.5194/acp-14-10963-2014 (2014).

Acknowledgements

This research has received funding from the European Commission's Seventh Framework Programme (FP7/2007–2013) through the European Research Council as ERC grant agreement 233366 (POPFULL) and through the People Programme/Marie Curie Actions as REA grant agreement PIIF-GA-2013-624245 (SRF-OZO). The modeling part was funded by the European Commission's Seventh Framework Programme project DESIRE (Development of a System of Indicators for a Resource Efficient Europe) as grant agreement 308552. We gratefully acknowledge the excellent technical support of Joris Cools, Jan Segers and Dr. Nicola Arriga as well as the logistic support of Kristof Mouton at the field site. We also thank Dr. Donatella Zona for the data processing of the O₃ fluxes, Dr. Silvano Fares and Dr. Flavia Savi for their help with the ozone flux partitioning.

Author Contributions

T.Z., C.H., F.B., E.F., B.G., M.P.-E., M.S. and R.C. T.Z. wrote the manuscript, analyzed the data. C.H. and M.S. ran the LOTUS Euros model, analyzed the data. F.B. conducted the measurements in the field. E.F. and B.G. analyzed the data and performed statistical analyses. M.P.-E. revised data and the manuscript text. R.C. provided framework and funding for the experimental field site, revised the data and the manuscript. All authors reviewed the manuscript.

Additional Information

Supplementary information accompanies this paper at <http://www.nature.com/srep>

Competing financial interests: The authors declare no competing financial interests.

How to cite this article: Zenone, T. *et al.* Interaction between isoprene and ozone fluxes in a poplar plantation and its impact on air quality at the European level. *Sci. Rep.* **6**, 32676; doi: 10.1038/srep32676 (2016).



This work is licensed under a Creative Commons Attribution 4.0 International License. The images or other third party material in this article are included in the article's Creative Commons license, unless indicated otherwise in the credit line; if the material is not included under the Creative Commons license, users will need to obtain permission from the license holder to reproduce the material. To view a copy of this license, visit <http://creativecommons.org/licenses/by/4.0/>

© The Author(s) 2016